



## UvA-DARE (Digital Academic Repository)

### Improving radiation dose delivery for moving targets using image guidance

Rooijen, D.C. van

**Publication date**  
2012

[Link to publication](#)

#### **Citation for published version (APA):**

Rooijen, D. C. V. (2012). *Improving radiation dose delivery for moving targets using image guidance*. [Thesis, fully internal, Universiteit van Amsterdam].

#### **General rights**

It is not permitted to download or to forward/distribute the text or part of it without the consent of the author(s) and/or copyright holder(s), other than for strictly personal, individual use, unless the work is under an open content license (like Creative Commons).

#### **Disclaimer/Complaints regulations**

If you believe that digital publication of certain material infringes any of your rights or (privacy) interests, please let the Library know, stating your reasons. In case of a legitimate complaint, the Library will make the material inaccessible and/or remove it from the website. Please Ask the Library: <https://uba.uva.nl/en/contact>, or a letter to: Library of the University of Amsterdam, Secretariat, P.O. Box 19185, 1000 GD Amsterdam, The Netherlands. You will be contacted as soon as possible.



## **Automatic Delineation of Body Contours on Cone-Beam CT Images Using a Delineation Booster**

Gjenna Stippel  
Dominique C van Rooijen  
Johannes Crezee  
Arjan Bel

Submitted

## 6.1 *Abstract*

In radiotherapy, cone-beam computerized tomography (CBCT) scans are used for position correction for various tumor sites. At the start of the treatment, a CT scan that serves as input for a treatment planning is acquired. At every fraction, a CBCT scan is made prior to the irradiation of the tumor. Because there might be significant interfractional tumor movement, on-line recalculation of the dose improves decision making on how to proceed.

A prerequisite for such recalculation is an accurately delineated body contour. In this note, we present an automatic delineation method for the body contour in the unprocessed CBCT scans, that employs a novel delineation boosting technique. The main idea of this technique is to construct an accurate delineation by combining the strength of several established but less accurate edge detectors in an innovative way. Quantitative validation reveals that the algorithm performs comparable with the manual delineations of two trained observers. Furthermore, because of the generic nature of the delineation boosting procedure, the algorithm can easily be extended with additional edge detectors to even further increase accuracy.

## 6.2 Introduction

Recently kilovoltage CBCT became widely available for routine clinical use in radiotherapy [19]. CBCT scans are used for position correction for various tumor sites, including the lung [35,82,83] and the pelvic area [69,72,84]. At the start of a treatment, a CT scan that serves as input for the treatment planning is acquired. Because of possible interfraction variation of the tumor position and set-up errors, a CBCT scan of the patient is made prior to the irradiation of the tumor. This provides a CT image with an image quality that is sufficient to verify the patient's position by bone or soft tissue matching, but is significantly worse than that of a regular CT image. The contrast is lower, hence soft tissue is poorly visible, and various reconstruction artifacts can deteriorate the image quality.

In the case that the anatomy of the patient has changed significantly with respect to the planning CT, e.g., because the patient lost weight or because of tumor movement, on-line recalculation of the dose might improve decision making on how to proceed. Use of CBCT for radiotherapy dose calculation is a rather novel concept. The accuracy of dose calculation depends critically on the accuracy of the reconstructed patient geometry. Regarding the internal anatomy, several solutions are proposed to deal with the inaccurate conversion of CBCT grey values to relative electron densities [65,72,74,76]. However, no attention is paid yet to an accurate delineation of the body outline. Such outlining is a nearly trivial task on conventional CT images whereby a grey-value threshold suffices. CBCT images on the other hand often suffer from artifacts with a blurred body surface, hampering the automatic delineation (figure 6.1). Other problems with CBCT are its limited field of view (often, part of the body is missing), and a rim-artifact present at the edge of the reconstruction circle.

Manual segmentation would allow a correction for these artifacts. In general, a human observer can easily distinguish the actual body contour. However, this task is labor intensive and too time-consuming for online dose recalculation. Presently there are no reports on automatic delineation of body contours on CBCT.

In this study, we present an automatic delineation method for the body contour in the unprocessed CBCT scans that employs a novel delineation boosting technique. Our technique is inspired on the Adaptive Boost (AdaBoost) algorithm, originally developed in the context of machine learning for classification of objects [85]. With the AdaBoost approach subsequent application of a number of classifiers converges to the correct result. Application of this scheme, with edge detectors as classifiers, is not yet reported for

segmenting CBCT images. In our study, this technique is implemented by combining the strength of several established but less accurate edge detectors. We also present a novel way to deal with artifacts and missing patient information.

The aim of this study is to find a robust algorithm for the delineation of body contours on CBCT images to enable radiotherapy dose calculations.

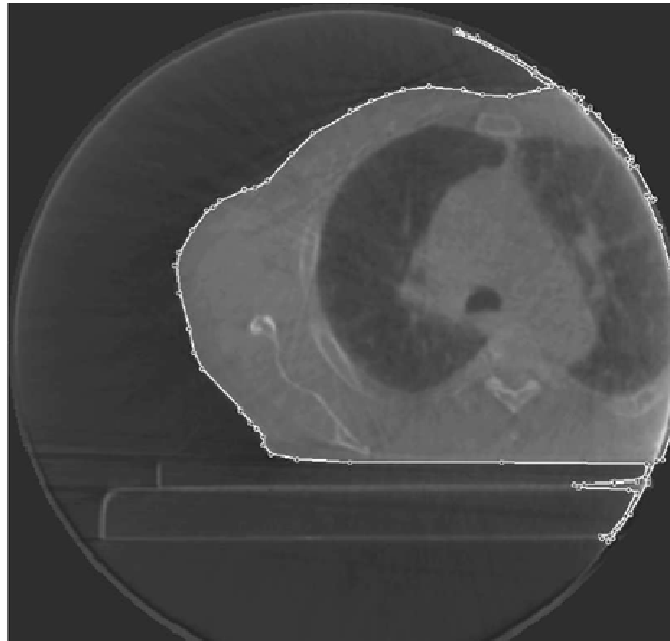


**Figure 6.1: Resulting contour with a standard contour tracking algorithm for regular CT images.**

### *6.3 Materials and Methods*

An overview of the entire algorithm is shown in figure 6.2. The algorithm consists of 4 steps and 2 preprocessing steps. In the following paragraphs, each step is discussed in detail. In step 1 and 2 we construct an initial delineation with a threshold based algorithm. In step 3 and 4, we boost the accuracy of this delineation by iteratively fine-tuning it with the result of a different classical edge detector at each iteration step.

#### **6.3.1 Preprocessing steps**

As a first preprocessing step, we select the subset  $U$  of all the slices of the scan for which the reconstruction circle covers a substantial part of the image. Because of the geometry of the scanner, the first and last few slices of the scan contain only a small region of useful data suitable for automatic interpretation. Rather than checking the slice numbers, however, we selected slices by checking whether the first 15 rows contain a pixel with a

value higher than that of the background. Due to this procedure, all tissue that requires radiation treatment will mostly be located in subset  $U$ .

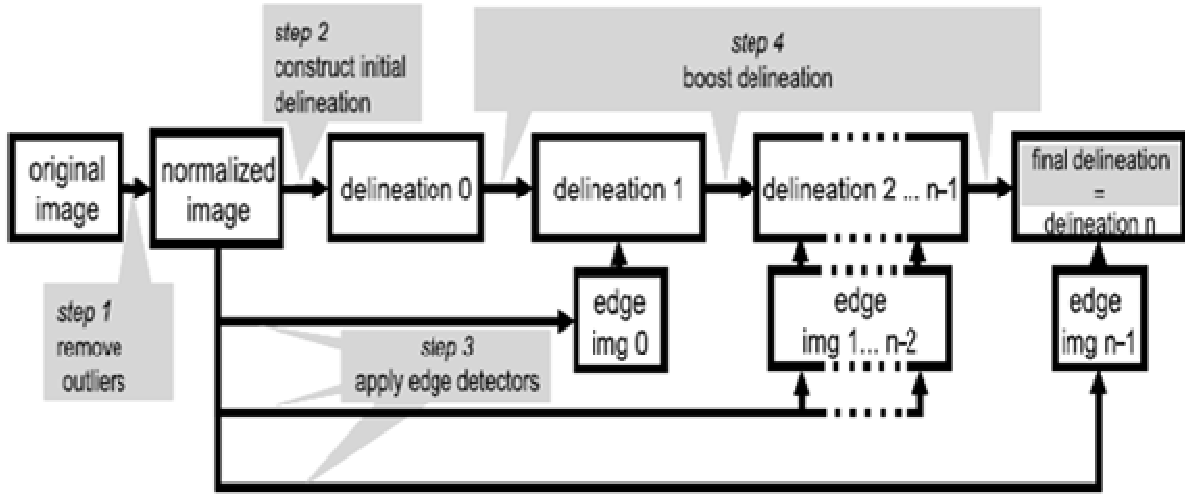


**Figure 6.2: Flow chart of the delineation boosting algorithm**

Secondly, we remove the region underneath the table by blackening out the rows below the average position of the treatment table top  $\tau_{top}$  in all slices of  $U$ . This position is found by performing edge detection with a Sobel edge detector [86] on all usable slices resulting in a collection  $E$  of binary edge images with 1 at the positions where the original image has large pixel level transitions (i.e., at the positions where an edge is detected) and 0 elsewhere.

Let  $v = (v_1, \dots, v_N)$  be an  $N$ -dimensional vector with  $N$  the number of rows of the images in  $E$ . Now let  $v_r$  be the frequency at which an edge is detected in the  $r$ th row of all images in  $E$ . The coefficient  $\lambda$  of the maximum element of  $v$ , i.e.,

$$\lambda = \arg \max_r v_r \quad (6.1)$$

indicates the row number in which an edge is detected in most images of  $E$ . Because the table top of the treatment table is a long horizontal edge at the same vertical position in almost all images of  $U$ , the position  $\tau_{top}$  equals  $\lambda$ . Finally, we fill all the rows of all images in  $U$  with row number  $\geq \tau_{top}$  with zeros.

After these preprocessing steps, we process each image in  $U$  with the delineation boosting algorithm, as displayed in figure 6.2.

### 6.3.2 Step 1: Remove outliers

We replace any extreme pixel values, due to artifacts or saturation, by a maximum value. This is necessary to be able to make a useful histogram, based on which we choose a threshold to create an initial delineation in step 2, and to ensure optimal performance of the edge detectors in step 3. An upper threshold  $\rho = \mu + 2.5\sigma$  is defined, where  $\mu$  is the average of the pixel values of the reconstruction circle in the original image  $A_{orig}$  and  $\sigma$  their standard deviation.

We replace the pixel values higher than  $\rho$  by  $\rho$  and obtain the normalized image  $A_{norm}$ . The definition of  $\rho$  is in accordance with the general statistical definition of an outlier in a data set.

### 6.3.3 Step 2: Construct an initial delineation

We construct an initial delineation of the body in  $A_{norm}$  by first making a threshold-based segmentation. Segmentation based on the grey value histogram is intricate because the histogram can be multi-modal due to streak-artifacts. For this purpose, we need to find a proper threshold value  $\Gamma$  and make a histogram  $H$  of 10 equally spaced bins of the pixel values of all pixels inside the reconstruction circle of  $A_{norm}$ . This number of bins ensures that  $H$  is nearly always bimodal, since the pixels in  $A_{norm}$  can be classified into two categories: the higher pixel values represent the various tissues, and the lower pixel values represent the air or low density tissue inside the body (e.g., lung) and outside the body.

Let  $\nu$  be the average of the 10 centre values of all bins of  $H$ . Denote the pixel value corresponding to the centre of the bin of the highest peak of  $H$  which is greater than  $\nu$  by  $\rho_{body}$  and the pixel value corresponding to the highest peak of  $H$  which is less than  $\nu$  by  $\rho_{backg}$ . Then we choose as a threshold  $\Gamma$  the average:

$$\Gamma = \frac{P_{body} + P_{backg}}{2} \quad (6.2)$$

We threshold the image  $A_{norm}$  at the value  $\Gamma$  and obtain the binary image  $\Sigma$ , containing one or more connected components (islands) among which the patient body. Because of the limited field of view, part of the body might fall outside the reconstruction circle. In this case it is not possible to outline the entire body contour and the delineating contour follows the edge of the reconstruction circle instead of the missing body contour. To facilitate this, we set the pixels of the background region outside the reconstruction circle in  $\Sigma$  to 1.

We fill the top 15 and the bottom 15 rows of the resulting image with 0-s and determine the region  $\Omega$  utilizing a region growing procedure that starts at the pixels in the top left-hand corner and the bottom right-hand corner of the image. After that, we take the complement of  $\Omega$ . Finally, we set the pixels of the background region outside the reconstruction circle to 0 again and set all pixels of the resulting binary image at 0 except those of the largest connected component. The result is a binary image of the body of the patient with any cavities filled. The collection of the exterior pixels of this connected component forms the initial delineating contour  $\Lambda_0$ .

### 6.3.4 Step 3: Apply the edge detectors

We apply a collection of  $n$  simple edge detectors on the image  $A_{norm}$  to obtain the  $n$  binary edge images  $B_0, \dots, B_{n-1}$ . In our case, we used the Sobel (1), the Prewitt (2), the Roberts (3), the Laplacian (4), the zero-cross (5) and the Canny edge detectors (6), respectively ( $n=6$ , where we refer for brevity to the numbers in the remainder) [86]. For each detector the standard settings were applied. Each of these edge detectors finds some parts of the body contour and misses other parts (because, e.g., the image is blurred at some places). If we combine the various edge images in the correct way, as we do in step 4, and include for each binary edge image the edges of the body in the delineating contour, the edge detectors enhance each other.

### 6.3.5 Step 4: Boost the delineation

In this step, we fine-tune the contour  $\Lambda_0$  using  $B_0$  with the boosting procedure  $\Phi$  described below and obtain  $\Lambda_1$ .

$$\Lambda_1 = \Phi(\Lambda_0 B_0) \quad (6.3)$$

Consider the binary edge image  $B_0$ . For this step, we only consider edges in  $B_0$  that cross (i.e., have at least one pixel in common with) the contour  $\Lambda_0$  and contain pixels of the region inside  $\Lambda_0$ .

The endpoints of these edges in  $B_0$  are found by starting at a pixel  $p_0$  where an edge  $E_0$  crosses  $\Lambda_0$  and scan its 8 adjacent pixels in clockwise order, starting at the top left pixel. If the pixel under consideration also belongs to  $B_0$ , then we call this pixel  $p_1$ . Subsequently, we scan  $p_1$ 's 8 adjacent pixels, etc. Proceeding like this, we 'walk' along the edge  $E_0$ . When we have arrived at  $p_r$  and do not find any new adjacent pixels that belong to  $B_0$ , we

identify  $p_r$  as being a terminus and continue with the next edge  $E_1$  in  $B_0$ . Once we are finished detecting all termini, we connect each terminus with a straight line to either another terminus or with a point of  $\Lambda_0$ , whichever is closer.

Finally, to regain one closed contour, we determine the central region with a region growing procedure, starting from the central pixel of the slice. Now, we remove all pixels drawn so far except the ones that are adjacent to  $\mathcal{O}$ . As a result, wherever  $B_0$  delineates the body more accurately than  $\Lambda_0$ , the parts of  $\Lambda_0$  are replaced by edges in  $B_0$ .

We repeat Step 4 for all  $n$  edge images  $B_0, \dots, B_{n-1}$ , thereby iteratively fine-tuning the delineating contour  $\Lambda_{m+1} = \Phi(\Lambda_m B_m)$ , where  $m = 0, \dots, n-1$ . In this way, we combined via an innovative boosting procedure the results of several simple edge detectors, to obtain an accurate delineation of the body.

The main idea is that each subsequent application of the edge detectors improves the outcome and the algorithm can in principle be extended with any number of detectors.

### 6.3.6 Performance analysis

We used 48 CBCT scans of patients treated for tumors in lung and pelvis in our department; 38 scans were of the thorax and 10 were of the pelvic area. The CBCTs were acquired with the Synergy system and registered with XVI release 3.5 (Elekta, Stockholm, Sweden). The 38 thorax scans were acquired with an M20 collimator, 360° scan, 120 kV and a bow-tie filter. Each of these scans consisted of 264 slices, slice thickness 1 mm. The 10 pelvic scans were acquired with an M10 collimator, 360° scan, 120 kV and a bow-tie filter. Each of these scans consisted of 120 slices, slice thickness 1 mm. The software that was used to write the algorithm to automatically produce the body contours was Matlab R2007b with the image processing toolbox extension (The Mathworks, Natick, MA, USA). The automatic delineations were performed on an Intel Dual Core CPU, E6850 @ 3.0 GHz and 1.96 GB of RAM (Intel, Santa Clara, CA, USA). The manual delineations that were used to evaluate the performance of the algorithm in terms of accuracy were made with the software package VolumeTool [87].

To evaluate the algorithm quantitatively, two trained observers delineated the body in our set of test scans. They only delineated the evenly numbered slices, since successive slices usually differ very little. One observer processed all 48 scans, the other 10 scans: 8 thorax scans and 2 pelvic scans. Moreover, we processed all scans automatically with our method and compared its results with the observer delineations using a method similar to the

method in Chai *et al* [88]: in every slice  $S$ , we calculated for each pixel  $p$  of the automatically generated contour the smallest distance  $k_p$  to the manual contour. Then we calculated the average  $\mu_S$  and the variance  $\nu_S$  of all  $k_p$  of the slice  $S$ , after which we calculated per scan the average  $M$  of the  $\mu_S$  and the average  $V$  of the  $\nu_S$  of all slices that had been delineated. The value of  $M$  can be interpreted as the average automatic-manual contour distance in the scan, and the value of  $\sqrt{V}$  as the average standard deviation of the automatic-manual contour distance. In a similar way the maximum deviations, averaged over all scans, were calculated. We calculated all this for the manual contours of both observers separately.

To demonstrate the benefit of the boosting method, we applied our method on the test set six times: the first time with one edge detector, the second time with two edge detectors etc. Then we calculated the average automatic-manual contour distance and the average standard deviation for the automatic-manual contour distance for all scans and both observers in all six cases. By randomly reordering four times, the filters for the analysis of the maximum deviation the efficacy of each filter could be revealed as well as if particular orders had effects on the end results.

Finally, we recorded the time it took the automatic method to delineate the scans and compared it with the time of the observers.

## 6.4 Results and Discussion

Figure 6.3 shows some examples of the resulting contour of applying 1 and 6 edge detectors.

The results for the averages of the mean shortest distances between the automatically delineated contours and the manual delineations of the observers are shown in figure 6.4. For all scans the average difference is smaller than 0.7 mm, and for almost all the scans the SD is smaller than 2 mm. Outliers with errors of 1.5 cm occurred in 1% of the slices; 1.9% of the errors were greater than 1 cm. Relatively high values for the average distance can be found for scan 1 and scan 38, and relatively high values for the average standard deviation can be found for scan 10, scan 29 and scan 38. In scan 1, 29 and 38, the body supporting board between the body and the table is erroneously enclosed in the contour by the algorithm in a number of slices which causes these high values. Since a tumor is generally not irradiated from this side, this is no obstacle to make a correct dose

recalculation. In scan number 10 the algorithm produces a wrong delineation because of the rim artifact at the edge of the reconstruction circle. Including more edge detectors reduces this effect though (see also figure 6.3).

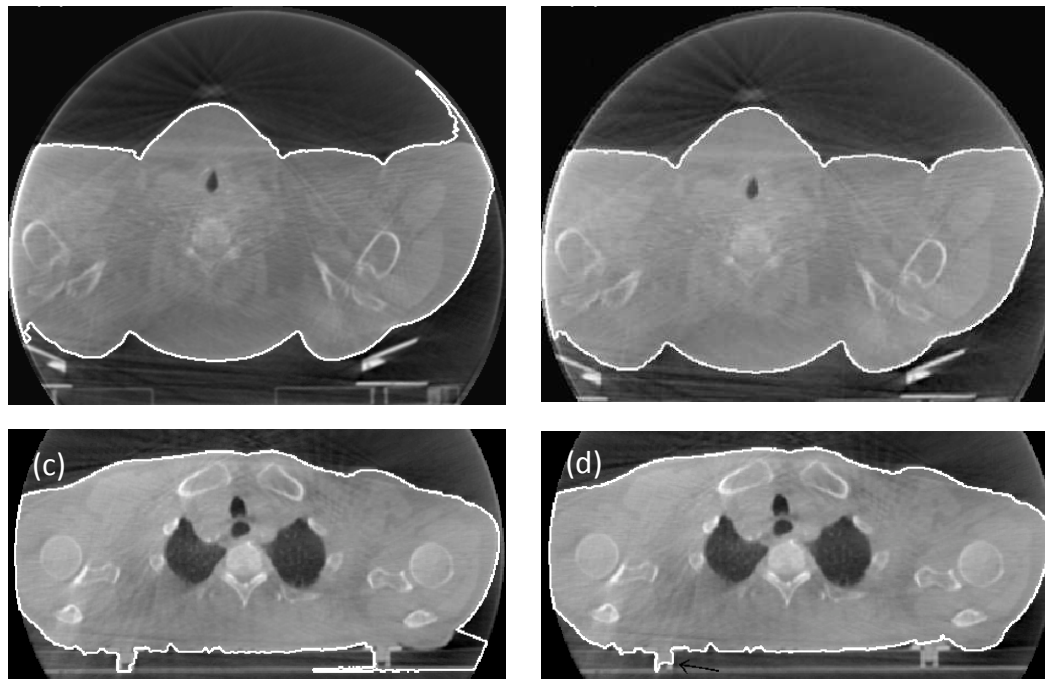


**Figure 6.3: Two slices of a CBCT scan and the results of the delineation boosting algorithm using 1 edge detector (a and c) and 6 edge detectors (b and d).**

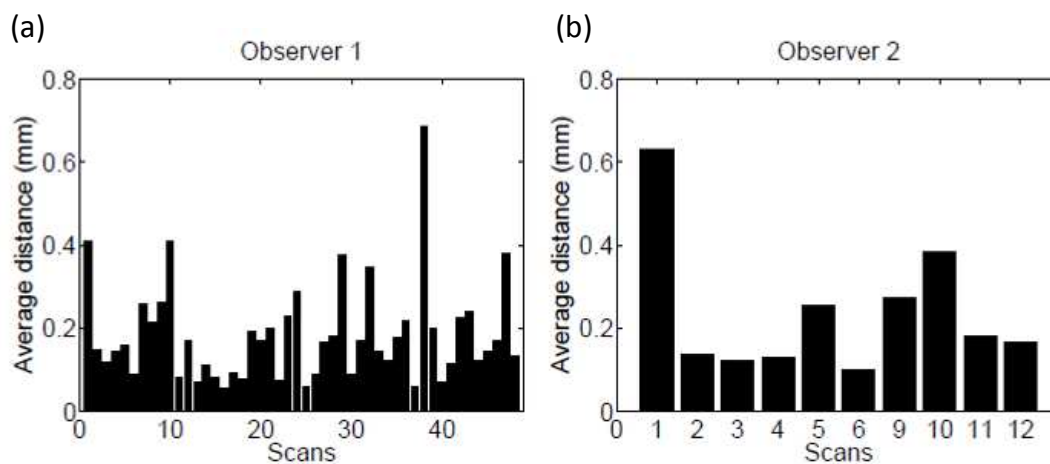


**Figure 6.4: The average of the mean shortest distances between the automatically delineated contours and the manual delineations per scan for both observers.**

Analysis of the average maximum deviation (figure 6.5) reveals that the overall performance of the algorithm improves for every extra edge detector we include. Depending on the order of the detectors, some detectors have less (or no) effect, probably because they detect basically the same edge features. The order used in this paper (i.e. 123456) ends up with the lowest errors but that same result can be achieved by

leaving out detector 4 or 5. Future work can include optimization of the number and order of detectors.

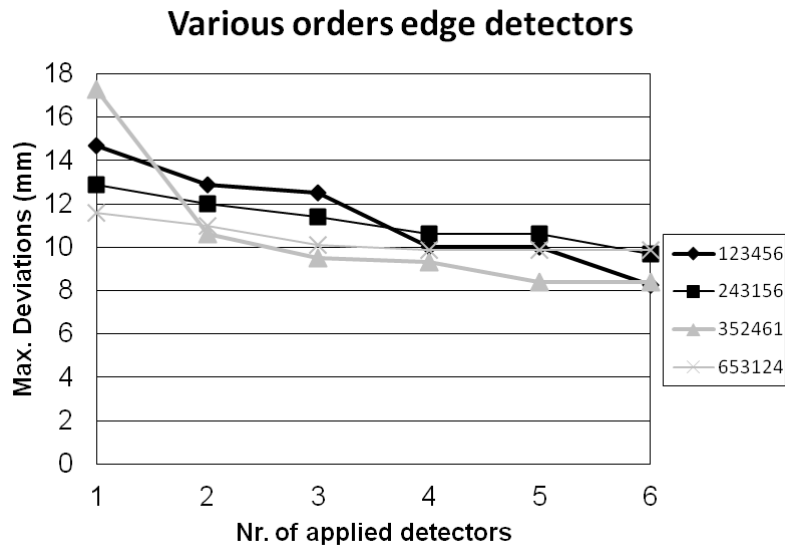


**Figure 6.5: Average of the maximum deviations for various orders of the edge detectors (denoted by their numbers, see section 6.3.4). Note that the order 123456 is used throughout the paper.**

Accurate application for radiotherapy planning of the automatic delineation is possible for the vast majority of cases. Errors in skin delineation of 1 – 1.5 cm occurred in less than 1% of the cases and yield dose errors of about 2.5% - 3.5% when a beam enters through that area. However, these type of errors are mainly caused by inclusion of (pieces of) the treatment couch (figure 6.3d). Such errors are local i.e. they typically occur in only a few consecutive slices. With a density corrected dose calculation consequences are very limited with modern carbon fiber table tops. Moreover, with a beam number of 5-7 for a radiotherapy plan, the errors will tend to cancel out. Errors with clear outliers greater than 1.5 cm are mostly due to the delineation ‘entering’ the body via an artifact (e.g., at the location of a metal artifact the delineating contour occasionally deviates from the outer surface of the body and delineates the inner lung contour instead). Such outliers deserve special attention. Pending a solution for these errors, human supervision of the results is mandatory.

Our method is derived from the AdaBoost technique [85]. The principle of AdaBoost states that an increasing number of classifiers yields a better performance. We did not rigidly prove the validity of AdaBoost but we have shown that the principle works for the type of problem in the present study. Including more than 6 edge detectors might yield further

improvement although some detectors might increase the accuracy more than others (figure 6.5).

Finally, the observers needed 41s on average to process one slice, while the algorithm needed 5.3s for it. Current investigation includes the conversion of the Matlab algorithm to C++. From this we expect further speedup of the process, allowing online computation.

### *6.5 Conclusion*

We successfully developed a technique that uses an innovative delineation boosting procedure to automatically and accurately delineate the body contour in CBCT scans used in radiotherapy.

#### **Acknowledgements**

We would like to thank Marlinde van Dijk and Donald Pool for outlining the body in all slices of the test scans and Prof. Aleksandra Piżurica for her helpful discussions.